JACS
JOURNAL OF THE AMERICAN CHEMICAL SOCIETY
Communication
pubs.acs.org/JACS

Enzyme-Instructed Assembly and Disassembly Processes for Targeting Downregulation in Cancer Cells

Zhaoqianqi Feng, Huaimin Wang, Rong Zhou, Jie Li, and Bing Xu*

Department of Chemistry, Brandeis University, 415 South Street, Waltham, Massachusetts 02454, United States

Supporting Information

ABSTRACT: Cancer cells differ from normal cells in both gain of functions (i.e., upregulation) and loss of functions (i.e., downregulation). While it is common to suppress gain of function for chemotherapy, it remains challenging to target downregulation in cancer cells. Here we show the combination of enzyme-instructed assembly and disassembly to target downregulation in cancer cells by designing peptidic precursors as the substrates of both carboxylesterases (CESs) and alkaline phosphatases (ALPs). The precursors turn into self-assembling molecules to form nanofibrils upon dephosphorylation by ALP, but CES-catalyzed cleavage of the ester bond on the molecules results in disassembly of the nanofibrils. The precursors selectively inhibit the cancer cells that downregulate CES (e.g., OVSAHO) but are innocuous to a hepatocyte that overexpresses CES (HepG2), while the two cell lines exhibit comparable ALP activities. This work illustrates a potential approach for the development of chemotherapy via targeting downregulation (or loss of functions) in cancer cells.

While the self-assembly of small molecules is a well-studied phenomenon in organic solvents[1] or on surfaces,[2] the formation of such structures in biological systems has only recently been described.[3−5] At the intersection of supramolecular chemistry and cell biology, supramolecular assemblies have shown great promise for cell cultures,[6] modulating immune responses,[7] delivering drugs,[8] inhibiting drug-resistant pathogens,[9] and inhibiting cancer cells.[10] We are particularly interested in the use of assemblies of molecules for cancer therapy because a serendipitous discovery[11] of the inverse comorbidity between cancer and neurodegenerative diseases implicates molecular nanofibrils formed by self-assembly in inhibiting cancer cells, either in an animal model[12] or in a human trial.[13] This notion, indeed, is supported by the development of enzyme-instructed self-assembly (EISA),[14] which selectively generates nanoscale assemblies of small molecules (e.g., small peptide derivatives[5,15,16] or carbohydrate derivatives[4]) in situ on cancer cells to inhibit the cancer cells.

EISA, as a process, differs fundamentally from the well-established prodrug approach[17] because in EISA only the assemblies, not the unassembled products of enzymatic conversion, are inhibitory to cancer cells.[15,18] Besides acting as a multiple-step process to inhibit cancer cells,[19] EISA promises an unprecedented way to target downregulation for cancer therapy, which remains a challenge in translational medicine. Scheme 1 shows the concept. A pair of cell lines both express alkaline phosphatase (ALP) at comparable levels, but one (e.g., OVSAHO) downregulates carboxylesterase (CES) while the other (e.g., HepG2) upregulates CES. Upon the action of ALP, the precursors turn into self-assembling molecules to form assemblies, but the assemblies dissociate upon the action of CES. Because the assemblies are cytotoxic and the unassembled products are innocuous to cells, the precursors would inhibit only the cells expressing ALP and downregulating CES. Thus, the overall result is to target the downregulation of the enzyme (e.g., CES) in cancer cells.

Scheme 1. Structures of the Precursor and Its Hydrolysis Products and the Concept of Targeting the Cells That Downregulate CES While Expressing ALP

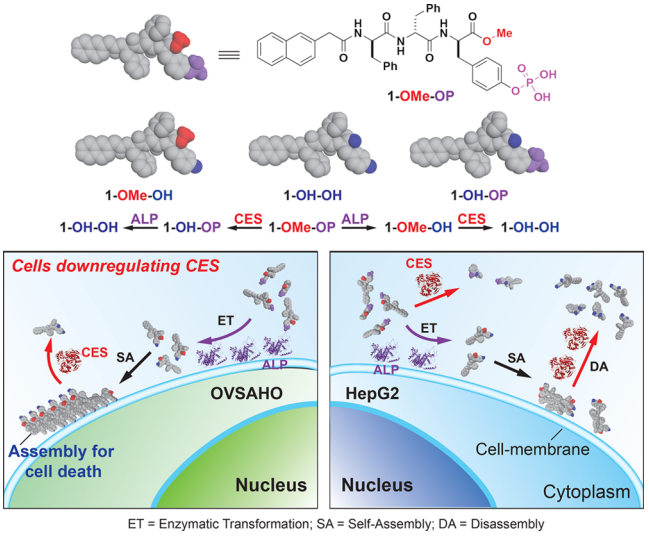

ET = Enzymatic Transformation; SA = Self-Assembly; DA = Disassembly

On the basis of the above concept, we designed the EISA precursor **1-OMe-OP**, which contains both a CES cleavage site (i.e., carboxyl methyl ester) and an ALP cleavage site (i.e., phosphotyrosine). Such a design allows ALP to convert **1-OMe-OP** to **1-OMe-OH**, CES to turn **1-OMe-OP** into **1-OH-OP**, and the actions of ALP and CES to generate **1-OH-OH**. Critical micelle concentration (CMC) and static light scattering (SLS) measurements revealed that **1-OMe-OH** favors self-assembly. Transmission electron microscopy (TEM) confirmed

Received: January 3, 2017
Published: March 3, 2017

DOI: 10.1021/jacs.7b00070
J. Am. Chem. Soc. 2017, 139, 3950−3953

that **1-OMe-OH**, generated by dephosphorylation of **1-OMe-OP**, forms nanofibrils and that CES catalyzes the dissociation of the nanofibrils by converting **1-OMe-OH** to **1-OH-OH**. Cell viability tests indicated that **1-OMe-OP** potently inhibits the cancer cells that downregulate CES (e.g., OVSAHO) but is innocuous to the cells that upregulate CES (e.g., HepG2), while those two cell lines exhibit comparable phosphatase activities. Control experiments (the addition of esterase inhibitors[20]) confirmed that the action and expression level of CES are critical for selectively inhibiting the cancer cells. A dicarboxyl methyl ester analogue of **1-OMe-OP** validated the generality of the concept. This work, for the first time, demonstrates the use of molecular assemblies to target the loss of function (i.e., an "untargetable" feature[21]) in cancer cells. Thus, it opens a new way for developing anticancer therapeutics based on the process of self-assembly and downregulation of enzymes.

The key feature of the design is that ALP-generated **1-OMe-OH** forms assemblies and the assemblies dissociate upon catalytic conversion of **1-OMe-OH** to **1-OH-OH** by CES. We synthesized the precursor **1-OMe-OP** and the relevant products (**1-OMe-OH**, **1-OH-OH**, and **1-OH-OP**) from its hydrolysis catalyzed by ALP or CES or both (Scheme 1). We first assessed their self-assembling abilities by measuring their CMCs. As shown in Figure 1A, the CMCs follow the order **1-OMe-OH** < **1-OMe-OP** < **1-OH-OH** < **1-OH-OP**. This result indicates that the presence of the phosphate group decreases the self-assembling ability of the Nap-capped tripeptide (Nap-ffy), while attaching methyl group to the C-terminus of Nap-ffy increases the self-assembling ability by about an order of magnitude. We used SLS to measure the signal change upon treatment of **1-OMe-OP** with ALP (Figure S13). The signal intensity ratio of the solution of **1-OMe-OP** (20 μM) was 0.3. The addition of ALP to that solution increased the ratio to 98.9, but the addition of CES decreased the ratio to 0.02. Moreover, incubating **1-OMe-OP** with ALP and CES together results in the formation of **1-OH-OH**, which exhibits a signal intensity ratio of 0.7, 2 orders of magnitude lower than that of **1-OMe-OH**. Agreeing with the CMC measurement, these results indicate that CES instructs the dissociation of the assemblies formed by ALP-instructed self-assembly of **1-OMe-OH**. In addition, the TEM images (Figure 1B) show that **1-OMe-OP** hardly forms any nanostructures at a concentration of 100 μM, while the addition of ALP results in the formation of nanofibrils with a diameter of 8 ± 2 nm. Upon coincubation with CES and ALP together, **1-OMe-OP** turns into **1-OH-OH**, which forms small particles with a diameter of 7 ± 2 nm. These TEM images confirm that ALP instructs the assembly of **1-OMe-OH** while CES catalyzes the dissociation of the assemblies.

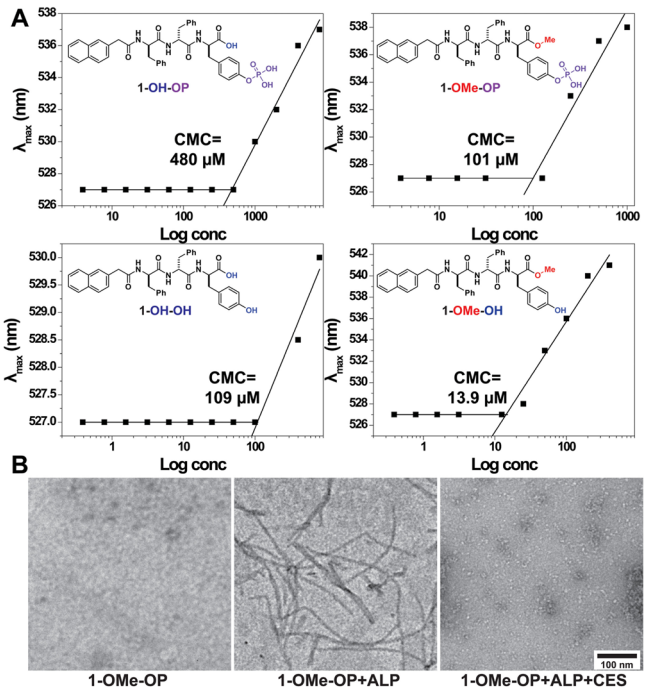

Figure 1. (A) CMC determination with rhodamine 6G for **1-OH-OP**, **1-OMe-OP**, **1-OH-OH**, and **1-OMe-OH**. (B) TEM images of the nanostructures formed by **1-OMe-OP** (100 μM) before and after the addition of ALP or both ALP and CES. In PBS (pH 7.4); scale bar = 100 nm.

To demonstrate the concept of targeting downregulation in cellular milieu, we chose OVSAHO, an ovarian cancer cell line, and HepG2 as a model cell of hepatocyte. According to the CCLE database, the mRNA expression of CES1 of HepG2 cells is nearly 3 times higher than that of OVSAHO cells, while these two cell lines express comparable levels of tissue-nonspecific alkaline phosphatase (ALPL) (Figure S14). Since the hydrolysis of the methyl ester bond in **1-OMe-OP** or **1-OMe-OH** is able to occur in pericellular space, we measured the activities of secreted esterases (eq S1) of HepG2 and OVSAHO cells in their conditioned media. As shown in Figure 2A, the relative activity (0.4) of the secreted esterases of HepG2 cells is almost 40 times higher than that of OVSAHO cells (0.01) at 8 h, indicating that HepG2 cells secrete more esterases than OVSAHO cells do. In the conditioned medium of HepG2 at 24 h, the relative activity of the secreted esterases (0.7) becomes about 5 times that of OVSAHO (0.14), suggesting that HepG2 cells constantly secrete more esterases than OVSAHO cells do.

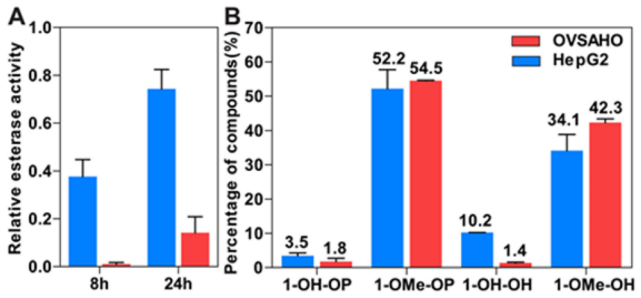

Figure 2. (A) Relative activities (compared to culture medium) of esterases secreted from the cells. (B) Percentage of the molecular species after incubation of **1-OMe-OP** (500 μM) with HepG2 or OVSAHO cells for 24 h.

We quantified the relevant conversion after incubating **1-OMe-OP** with HepG2 or OVSAHO cells for 24 h (Figure 2B). LC–MS analysis indicated that only about 50% of the precursor (**1-OMe-OP**) remained in both types of cells (i.e., 44.3% for HepG2 and 44.2% for OVSAHO), indicating that HepG2 and OVSAHO in fact exhibit comparable phosphatase activities. However, the CES from HepG2 hydrolyzes 14% of the carboxyl methyl ester, which is 4 times higher than the amount CES from OVSAHO hydrolyzes (i.e., 3.2%). Although the difference of **1-OMe-OH** in HepG2 and OVSAHO is only about 8%, the **1-OMe-OH**/**1-OH-OH** molar ratios in the

DOI: 10.1021/jacs.7b00070
J. Am. Chem. Soc. 2017, 139, 3950–3953

cultures of HepG2 and OVSAHO are 3.3 and 30, respectively. Thus, we speculate that **1-OH-OH** likely promotes the disassembly of **1-OMe-OH**. Congo red, a dye for self-assembled nanofibrils,[15] helped us directly visualize the formation of nanofibrils in the pericellular space of OVSAHO and HepG2 cells (Figure S15). Moreover, the pericellular fluorescence deceased upon washing, agreeing with the idea that the nanofibrils form on the cell surface. The confocal images also reveal that more nanofibrils formed on OVSAHO cells than on HepG2 cells, agreeing with the cell viability results. These results, which agree with the enzyme expression levels and the relative activities of the secreted esterases of the cells, further support the design for targeting cells that downregulate CES (Scheme 1).

While **1-OMe-OP** potently inhibits OVSAHO cells at 50 μM (Figure 3A), it is almost innocuous to HepG2 cells. The IC_{50} value of **1-OMe-OP** against HepG2 cells (338 μM) is about 15 times higher than that against OVSAHO cells (22 μM), confirming that **1-OMe-OP** selectively targets OVSAHO cells. Besides the difference in their self-assembling abilities, the carboxylic species (e.g., **1-OH-OH**) likely adheres less to the cell membrane than does the methyl ester one (e.g., **1-OMe-OH**) and thus exhibits less cytotoxicity. To prove further that CES hydrolysis contributes to the low cytotoxicity of **1-OMe-OP** against HepG2, we coincubated CES inhibitors and **1-OMe-OP** with HepG2 (Figure 3B). The addition of troglitazone (a CES1 inhibitor[20]) or loperamide (a CES2 inhibitor[22]) reduced the IC_{50} of **1-OMe-OP** against HepG2 from 338 μM to 133 μM and 117 μM, respectively. BNPP (an inhibitor of both CES1 and CES2[23]) lowered the IC_{50} of **1-OMe-OP** against HepG2 by almost an order of magnitude (from 338 μM to 43 μM). In agreement with the fact that HepG2 cells express both CES1 and CES2,[24] the inhibition of CES reduces the hydrolysis of **1-OMe-OH**, thus boosting the cytotoxicity of **1-OMe-OP** toward HepG2. In contrast, the addition of troglitazone hardly shows any effect on the viability of OVSAHO cells, and BNPP or loperamide only slightly decreases the IC_{50} value of **1-OMe-OP** against OVSAHO cells (Figures 3B and S17). These results confirm that **1-OMe-OP** is able to target the downregulation of CES in OVSAHO cells.

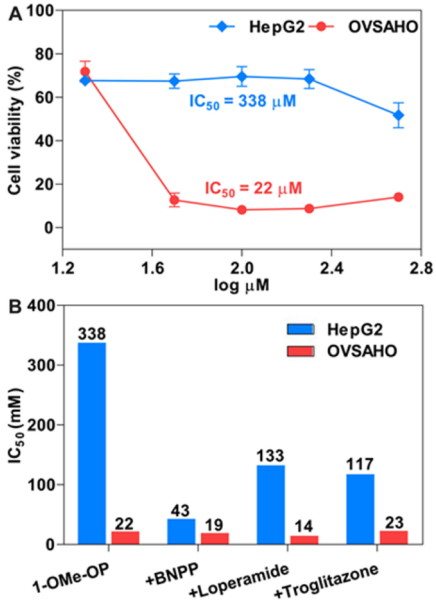

Figure 3. (A) Viabilities of HepG2 and OVSAHO cells treated with **1-OMe-OP**. (B) IC_{50} values (at 72 h) of **1-OMe-OP** against HepG2 or OVSAHO cells without/with addition of the inhibitors of esterases: BNPP (nonspecific), loperamide (CES2), and troglitazone (CES1).

To verify the generality of the concept in Scheme 1, we developed **2-$(OMe)_2$-OP** (Figure 4A), a dicarboxyl methyl ester analogue of **1-OMe-OP**, as another precursor (Scheme S2). Upon the action of ALP, **2-$(OMe)_2$-OP** turns into **2-$(OMe)_2$-OH**, which self-assembles in water to form nanotubes with a diameter of 14 ± 2 nm (Figures S19 and S20). Similar to **1-OMe-OH**, **2-$(OMe)_2$-OH** becomes **2-$(OH)_2$-OH** upon the action of CES. The CMCs (Figure S21) follow the order **2-$(OMe)_2$-OH** (2.66 μM) < **2-$(OMe)_2$-OP** (30.4 μM) < **2-$(OH)_2$-OH** (112 μM) < **2-$(OH)_2$-OP** (500 μM). Cell assays confirmed that **2-$(OMe)_2$-OP** selectively inhibits OVSAHO over HepG2, exhibiting IC_{50} values of 5 μM against OVSAHO cells and over 200 μM against HepG2 cells (Figure 4B). Notably, the IC_{50} of **2-$(OMe)_2$-OP** is 4.4 μg/mL, which is comparable to that of cisplatin (5.5 μg/mL[25]) against OVSAHO in cell assays. Besides supporting the idea that the molecular design of the substrates of ALP and CES (Scheme 1) is a general strategy, this result, together with the results for **1-OMe-OP**, further validate the approach of targeting the downregulation of CES in cancer cells by enzyme-instructed assembly and disassembly processes.

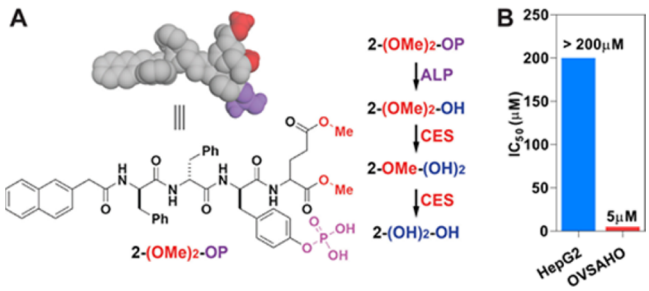

Figure 4. (A) Molecular structure and enzymatic conversion of the precursor **2-$(OMe)_2$-OP**. (B) IC_{50} values (at 72 h) of **2-$(OMe)_2$-OP** against HepG2 or OVSAHO cells.

In conclusion, this work demonstrates that the combination of enzyme-instructed assembly and disassembly is able to target downregulation (or loss of functions) in cancer cells. The results reported here would be particularly beneficial for treating metastatic cancers, where the cancerous cells exist alongside healthy cells (e.g., metastatic ovarian cancer into liver[26]). Notably, the IC_{50} values of the precursors against OVSAHO cells follow the lowest CMCs of the corresponding hydrolysis products (Figure S22), indicating that the CMC values may help predict the effective concentrations of the precursors in cell assays. Interestingly, although the mRNA expression of ALPL in OVSAHO cells is slightly higher than that in HepG2 cells, the two cell lines exhibit comparable phosphatase activities toward the precursors, which underscores the need to validate the enzyme activities experimentally for precise targeting of cancer cells. Although this work used ALP and CES, the principle demonstrated here should be applicable to any other enzymes[27] or cellular difference,[28] especially the difference in loss of functions, for spatiotemporal control of molecular assemblies that control cell fate.

DOI: 10.1021/jacs.7b00070
J. Am. Chem. Soc. 2017, 139, 3950−3953

■ ASSOCIATED CONTENT

Supporting Information

The Supporting Information is available free of charge on the ACS Publications website at DOI: 10.1021/jacs.7b00070.

Synthetic procedures, characterizations, and cell viability (PDF)

■ AUTHOR INFORMATION

Corresponding Author

*bxu@brandeis.edu

ORCID

Huaimin Wang: 0000-0002-8796-0367

Bing Xu: 0000-0002-4639-387X

Notes

The authors declare no competing financial interest.

■ ACKNOWLEDGMENTS

This work was partially supported by NIH (R01CA142746) and NSF (MRSEC-1420382).

■ REFERENCES

(1) Terech, P.; Weiss, R. G. *Chem. Rev.* **1997**, *97*, 3133. Ikeda, A.; Shinkai, S. *Chem. Rev.* **1997**, *97*, 1713. Sangeetha, N. M.; Maitra, U. *Chem. Soc. Rev.* **2005**, *34*, 821. Lehn, J.-M. *Proc. Natl. Acad. Sci. U. S. A.* **2002**, *99*, 4763. Whitesides, G. M.; Mathias, J. P.; Seto, C. T. *Science* **1991**, *254*, 1312.

(2) Love, J. C.; Estroff, L. A.; Kriebel, J. K.; Nuzzo, R. G.; Whitesides, G. M. *Chem. Rev.* **2005**, *105*, 1103.

(3) Yang, Z.; Xu, K.; Guo, Z.; Guo, Z.; Xu, B. *Adv. Mater.* **2007**, *19*, 3152. Zorn, J. A.; Wille, H.; Wolan, D. W.; Wells, J. A. *J. Am. Chem. Soc.* **2011**, *133*, 19630. Kato, M.; Han, T. N. W.; Xie, S. H.; Shi, K.; Du, X. L.; Wu, L. C.; Mirzaei, H.; Goldsmith, E. J.; Longgood, J.; Pei, J. M.; Grishin, N. V.; Frantz, D. E.; Schneider, J. W.; Chen, S.; Li, L.; Sawaya, M. R.; Eisenberg, D.; Tycko, R.; McKnight, S. L. *Cell* **2012**, *149*, 753.

(4) Pires, R. A.; Abul-Haija, Y. M.; Costa, D. S.; Novoa-Carballal, R.; Reis, R. L.; Ulijn, R. V.; Pashkuleva, I. *J. Am. Chem. Soc.* **2015**, *137*, 576.

(5) Tanaka, A.; Fukuoka, Y.; Morimoto, Y.; Honjo, T.; Koda, D.; Goto, M.; Maruyama, T. *J. Am. Chem. Soc.* **2015**, *137*, 770.

(6) Silva, G. A.; Czeisler, C.; Niece, K. L.; Beniash, E.; Harrington, D. A.; Kessler, J. A.; Stupp, S. I. *Science* **2004**, *303*, 1352.

(7) Rudra, J. S.; Tian, Y. F.; Jung, J. P.; Collier, J. H. *Proc. Natl. Acad. Sci. U. S. A.* **2010**, *107*, 622. Wang, H. M.; Luo, Z.; Wang, Y. C. Z.; He, T.; Yang, C. B.; Ren, C. H.; Ma, L. S.; Gong, C. Y.; Li, X. Y.; Yang, Z. M. *Adv. Funct. Mater.* **2016**, *26*, 1822.

(8) Zhao, F.; Ma, M. L.; Xu, B. *Chem. Soc. Rev.* **2009**, *38*, 883. Cheetham, A. G.; Zhang, P.; Lin, Y.-a.; Lock, L. L.; Cui, H. *J. Am. Chem. Soc.* **2013**, *135*, 2907.

(9) Salick, D. A.; Kretsinger, J. K.; Pochan, D. J.; Schneider, J. P. *J. Am. Chem. Soc.* **2007**, *129*, 14793. Xing, B. G.; Yu, C. W.; Chow, K. H.; Ho, P. L.; Fu, D. G.; Xu, B. *J. Am. Chem. Soc.* **2002**, *124*, 14846.

(10) Julien, O.; Kampmann, M.; Bassik, M. C.; Zorn, J. A.; Venditto, V. J.; Shimbo, K.; Agard, N. J.; Shimada, K.; Rheingold, A. L.; Stockwell, B. R.; Weissman, J. S.; Wells, J. A. *Nat. Chem. Biol.* **2014**, *10*, 969.

(11) Driver, J. A.; Beiser, A.; Au, R.; Kreger, B. E.; Splansky, G. L.; Kurth, T.; Kiel, D. P.; Lu, K. P.; Seshadri, S.; Wolf, P. A. *Br. Med. J.* **2012**, *344*, e1442.

(12) Gallardo, R.; Ramakers, M.; De Smet, F.; Claes, F.; Khodaparast, L.; Khodaparast, L.; Couceiro, J. R.; Langenberg, T.; Siemons, M.; Nystrom, S.; Young, L. J.; Laine, R. F.; Young, L.; Radaelli, E.; Benilova, I.; Kumar, M.; Staes, A.; Desager, M.; Beerens, M.; Vandervoort, P.; Luttun, A.; Gevaert, K.; Bormans, G.; Dewerchin, M.; Van Eldere, J.; Carmeliet, P.; Vande Velde, G.; Verfaillie, C.; Kaminski, C. F.; De Strooper, B.; Hammarstrom, P.; Nilsson, K. P. R.; Serpell, L.; Schymkowitz, J.; Rousseau, F. *Science* **2016**, *354*, aah4949.

(13) Gustafsson, L.; Leijonhufvud, I.; Aronsson, A.; Mossberg, A.-K.; Svanborg, C. *N. Engl. J. Med.* **2004**, *350*, 2663.

(14) Du, X.; Zhou, J.; Shi, J.; Xu, B. *Chem. Rev.* **2015**, *115*, 13165.

(15) Kuang, Y.; Shi, J.; Li, J.; Yuan, D.; Alberti, K. A.; Xu, Q.; Xu, B. *Angew. Chem., Int. Ed.* **2014**, *53*, 8104.

(16) Wang, H.; Feng, Z.; Wu, D.; Fritzsching, K. J.; Rigney, M.; Zhou, J.; Jiang, Y.; Schmidt-Rohr, K.; Xu, B. *J. Am. Chem. Soc.* **2016**, *138*, 10758. Feng, Z.; Wang, H.; Du, X.; Shi, J.; Li, J.; Xu, B. *Chem. Commun.* **2016**, *52*, 6332. Li, J.; Kuang, Y.; Shi, J. F.; Zhou, J.; Medina, J. E.; Zhou, R.; Yuan, D.; Yang, C. H.; Wang, H. M.; Yang, Z. M.; Liu, J. F.; Dinulescu, D. M.; Xu, B. *Angew. Chem., Int. Ed.* **2015**, *54*, 13307. Wang, H. M.; Feng, Z. Q. Q.; Wang, Y. Z.; Zhou, R.; Yang, Z. M.; Xu, B. *J. Am. Chem. Soc.* **2016**, *138*, 16046.

(17) Rautio, J.; Kumpulainen, H.; Heimbach, T.; Oliyai, R.; Oh, D.; Jaervinen, T.; Savolainen, J. *Nat. Rev. Drug Discovery* **2008**, *7*, 255. Brunton, L.; Hilal-Dandan, R.; Goodman, L. S. *Goodman and Gilman Manual of Pharmacology and Therapeutics*; McGraw Hill Professional: New York, 2013.

(18) Shi, J.; Du, X.; Yuan, D.; Zhou, J.; Zhou, N.; Huang, Y.; Xu, B. *Biomacromolecules* **2014**, *15*, 3559.

(19) Zhou, J.; Xu, B. *Bioconjugate Chem.* **2015**, *26*, 987.

(20) Fu, J.; Sadgrove, M.; Marson, L.; Jay, M. *Drug Metab. Dispos.* **2016**, *44*, 1313.

(21) Bourzac, K. *Nature* **2014**, *509*, S69.

(22) Quinney, S. K.; Sanghani, S. P.; Davis, W. I.; Hurley, T. D.; Sun, Z.; Murry, D. J.; Bosron, W. F. *J. Pharmacol. Exp. Ther.* **2005**, *313*, 1011.

(23) Ohura, K.; Sakamoto, H.; Ninomiya, S.-i.; Imai, T. *Drug Metab. Dispos.* **2010**, *38*, 323.

(24) Ross, M. K.; Borazjani, A.; Wang, R.; Crow, J. A.; Xie, S. *Arch. Biochem. Biophys.* **2012**, *522*, 44.

(25) Elias, K. M.; Emori, M. M.; Papp, E.; MacDuffie, E.; Konecny, G. E.; Velculescu, V. E.; Drapkin, R. *Gynecol. Oncol.* **2015**, *139*, 97.

(26) Lengyel, E. *Am. J. Pathol.* **2010**, *177*, 1053.

(27) Dragulescu-Andrasi, A.; Kothapalli, S. R.; Tikhomirov, G. A.; Rao, J. H.; Gambhir, S. S. *J. Am. Chem. Soc.* **2013**, *135*, 11015. Jiang, T.; Olson, E. S.; Nguyen, Q. T.; Roy, M.; Jennings, P. A.; Tsien, R. Y. *Proc. Natl. Acad. Sci. U. S. A.* **2004**, *101*, 17867.

(28) Zheng, Z.; Chen, P.; Xie, M.; Wu, C.; Luo, Y.; Wang, W.; Jiang, J.; Liang, G. *J. Am. Chem. Soc.* **2016**, *138*, 11128.

DOI: 10.1021/jacs.7b00070
J. Am. Chem. Soc. 2017, 139, 3950−3953